RSC Advances

This article can be cited before page numbers have been issued, to do this please use: J. Ki, A. Mukherjee, S. Rangasamy, B. Purushothaman and J. M. Song, *RSC Adv.*, 2016, DOI: 10.1039/C6RA11111D.

ROYAL SOCIETY OF CHEMISTRY

www.rsc.org/advances

View Article Online
DOI: 10.1039/C6RA11111D

Insulin-mimetic and Anti-inflammatory Potential of a Vanadyl-Schiff Base Complex for its Application against Diabetes

Jieun Ki†, Abhishek Mukherjee†, Sabarinathan Rangasamy†, Baskaran Purushothaman and Joon Myong Song*

College of Pharmacy, Seoul National University, Seoul 151-742, South Korea

* Corresponding author

Prof. Joon Myong Song,

College of Pharmacy, Seoul National University, Seoul 151-742, South Korea

Tel: +82 2 880 7841; Fax: + 82 2 871 2238

E-mail: jmsong@snu.ac.kr (Joon Myong Song)

†These authors contributed equally to this work.

View Article Online
DOI: 10.1039/C6RA11111D

Abstract

Insulin signalling causes the translocation of glucose transporter 4 (GLUT4) to the plasma membrane to facilitate cellular glucose uptake. Numerous observations indicate that the prime cause of type 2 diabetes mellitus (T2DM) is inflammation, the occurrence of which increases in obese individuals. Inflammatory mediators induce an insulin-resistance (IR) state where impaired insulin signalling fails to promote the glucose transporters for intracellular uptake of glucose. Hence compounds, which possess insulin-mimetic and anti-inflammatory potentials, may be effective in the treatment of obesity-induced IR during T2DM. Previous studies showed that vanadium oxo complexes possess insulin-mimetic activities whereas tryptamine moiety offers anti-inflammatory potential. Hence a vanadyl-Schiff base complex (VOTP) consisting of the tryptamine moiety was synthesized by condensation of pyridoxal hydrochloride and tryptamine and its subsequent complexation with $VOSO_4$. HEK-293 cells, expressing a GLUT4-myc-GFP fusion protein, were treated with VOTP and GLUT4 translocation was quantified by total internal reflection fluorescence (TIRF) microscopy. Results indicated that VOTP could efficiently act as an insulin-mimetic substance. High-content cell based assay using quantum dot-antibody conjugates showed that VOTP restored insulin signaling during IR by the inactivation of c-Jun N-terminal kinase-1 (JNK-1) and subsequent phosphorylation and activation of tyrosine moiety of insulin receptor substrate (IRS). Also, high levels of phosphorylated Forkhead box O1 (FOXO) indicated low levels of gluconeogenesis. Hence VOTP has insulin-mimetic and anti-inflammatory potentials. Moreover, VOTP is highly effective at nanomolar treatment ranges, thus evades the toxicity issues. Collectively, these findings encourage us for future use of this compound as a potential anti-diabetic agent.

View Article Online
DOI: 10.1039/C6RA11111D

Keywords: Insulin resistance; glucose transporter 4; total internal reflection fluorescence; inflammation; bifunctional vanadium (IV) complex.

Abbreviation list

GLUT4: Glucose transporter 4; T2DM: Type 2 diabetes mellitus; IR: Insulin resistance; TIRF: Total internal reflection fluorescence; JNK: c-Jun N-terminal kinase-1; IRS: Insulin receptor substrate; FOXO: Forkhead box O1; TNF-α: Tumor necrosis factor alpha; DMEM: Dulbecco's modified Eagle's medium; 2-NBDG: 2-[N-(7-nitrobenz-2-oxa-1, 3-diazol-4-yl)amino]-2- deoxy-D-glucose; GSK: Glycogen synthase kinase; PI3K: Phosphatidylinositol-3-kinase; IRSTK: IRS tyrosine kinase.

View Article Online
DOI: 10.1039/C6RA11111D

Introduction

The inability of cells to respond to insulin signalling is defined as insulin resistance (IR), which constitutes the characteristic feature of type 2 diabetes mellitus (T2DM). The chronic inflammatory response plays the key role in reduced insulin sensitivity. Patients suffering from T2DM are often diagnosed with high levels of tumor necrosis factor alpha (TNF-α). Recent reports implicated TNF-α as the major pro-inflammatory cytokine responsible for the pathogenesis of insulin resistance.[1] Insulin-stimulated glucose disposal is markedly reduced with increased expression of TNF-α.[2] TNF-α inhibits the phosphorylation of insulin receptor tyrosine by impeding tyrosine kinase of IRS-1, thus inhibiting insulin signalling.[3] General therapeutic approaches include anti-inflammation-based combination to overcome inflammation and reduced sensitivity to insulin. Accordingly, a compound possessing both anti-inflammatory and insulin mimetic properties could contribute greatly to the achievement of efficient antidiabetic therapies. A single compound with bifunctional therapeutic activity is very advantageous for reducing the entire dose and improving the ease of drug formulation.

Regulation of glucose transporters (GLUT) constitutes another mode of TNF-α -induced insulin resistance.[4] GLUT proteins are glucose carriers that, upon insulin signalling, mediate the facilitated diffusion of glucose down the concentration gradient inside of cells. Most of those transporters reside on the cell membrane. However, GLUT4 is located in intracellular vesicles in the basal state, either sequestered or inactive, and is translocated to the plasma membrane upon insulin signalling to facilitate glucose uptake by cells.[5] TNF-α is found to be associated with low GLUT-4 expression levels and

View Article Online
DOI: 10.1039/C6RA11111D

inhibits insulin-stimulated GLUT4 translocation.[6, 7] Impaired GLUT4 translocation is believed to be the major cause of insulin resistance.

Vanadium oxo (VO) complexes, with improved solubility and reduced cytotoxicity, are promising agents for the treatment of T2DM, as they possess insulin-mimetic properties. The mechanism involves enhanced tyrosine phosphorylation in IRS and enhancement in insulin-stimulated GLUT4 translocation.[8] Vanadyl (VO^{2+}) is preferred to vanadate (VO_4^{3-}) for use as an insulin-mimetic agent, as the former is less toxic to living cells.

The assessment of GLUT4 translocation poses a major challenge as GLUT4 cannot be detected directly. Indirect methods, such as Western blot, ELISA, and immunoelectron microscopic techniques are non-sensitive, time-consuming, and cannot produce quantitative data.[9] Alternatively, different epitope tags and genetically encoded fluorophores have been attached with GLUT4 for investigation of its cellular localization and translocation.[10] Evanescent field microscopy, commonly known as total internal reflection fluorescence (TIRF) microscopy, constitutes an effective technique to selectively excite and visualize fluorophores, as the evanescent angle restricts the imaging of intracellular regions. TIRF allows imaging only near the plasma membrane and minimizes background fluorescence, thus providing images with a higher signal-to-noise ratio in comparison to those obtained in conventional epifluorescence studies. The technique is efficient in quantifying the extent of protein translocation.

Until now, reports are scanty regarding a complex with insulin-mimetic and anti-inflammatory roles together, for its potential use during the IR state. Such a complex with bifunctional activities could be a suitable alternative due to its low dosage frequency in comparison to combination therapy. Here, we report a novel bifunctional vanadyl-Schiff

View Article Online
DOI: 10.1039/C6RA11111D

base complex (VOTP). TIRF was applied to quantify the translocation of GLUT4 to the plasma membrane during an inflammation-induced IR state by TNF-α treatment in HEK-293cells (Fig. 1A). The synthesized VOTP was applied to the inflammation-induced IR cell-based assay using TIRF in order to assess its bifunctional potential to act as an anti-inflammatory agent and insulin-mimetic molecule in maintaining normal glucose homeostasis during TNF-α induced inflammation and IR.

Materials and Methods

Plasmid Construct and Chemicals

The pB-GLUT4myc7-GFP construct was purchased from Addgene (MA, USA). Human insulin, wortmannin, glucose assay kit, and TNF-α were purchased from Sigma-Aldrich (St. Louis, MO, USA). Vanadium (IV) oxide sulfate hydrate was purchased from Sigma-Aldrich Korea. Pyridoxal hydrochloride, Sodium acetate and tryptamine were purchased from Alfa-Aesar. All solvents were purchased from Sigma-Aldrich Korea.

Synthesis of Schiff base Ligand (TPL)

TPL (Fig 1B (i)) was synthesized according to a previously described method.[11] Pyridoxal hydrochloride (0.5 mM) and tryptamine (0.5 mM) were dissolved in dry ethanol, stirred and refluxed for 3 h under N_2 atmosphere, and then the solvent was removed under reduced pressure using a rotary evaporator. The product was precipitated by the addition of acetonitrile. The precipitate was collected and dried under vacuum. Yield: 50%. Anal. Calcd for $C_{18}H_{19}N_3O_2$: C, 69.88; H, 6.19; N, 13.58; O, 10.34; Found: C, 69.34; H, 6.56; N, 13.73; O, 10.28. Selected IR peaks with tentative assignments (ν_{max}, cm^{-1}): 3457 (O–H), 2963 (C–H), 1635 (C═N Schiff base coupled to the aromatic ring), 1011 (C–O

View Article Online
DOI: 10.1039/C6RA11111D

phenol). FAB-MS: 310 [M+1]. ^{1}H NMR (DMSO-d6, δ/ppm): 2.37 (3H, s, CH_3), 4.75 (4H, s, CH_2 attached to OH), 7.24 (1H, s, CH), 7.26 (1H, s, CH), 7.95 (1H, s, CH=N), 10.4 (1H, s, NH), ^{13}C NMR (500 MHz, DMSO-d6, δ/ppm): 136.26, 126.77, 123.22, 121.11, 118.96, 118.41, 118.04, 111.49, 58.48, 23.05, 19.62, 17.94.

Synthesis of bis(pyridoxylidenetryptamine) vanadium(IV) complex (VOTP)

VOTP was prepared by refluxing a mixture containing 0.5 mM of TPL and 0.25 mM of $VOSO_4$ in dry methanol for 15 h. Briefly 0.25 mM of tryptamine and 0.25 mM of pyridoxal hydrochloride were taken in a round-bottom flask, and 10 ml of dry methanol was added. The reaction mixture was refluxed at 70^{0}C for 3 h. The Schiff base ligand formation (TPL) was confirmed by using TLC. 0.25 mM of $VOSO_4$ was then dissolved in 5 ml of hot methanolic solution, and then added dropwise to the above ligand solution. Finally, sodium acetate (1mM) was added. Heating continued for 12 h under N_2 atmosphere. The excess solvent was removed using a rotary evaporator. The green color solid (VOTP complex) was isolated and washed with diethyl ether and hexane. The compound was dried under a vacuum condition and stored at 4^{0}C. Yield: 50%. Anal. Calcd for $C_{36}H_{36}N_6O_5V$: C, 63.25; H, 5.31; N, 12.29; Found: C, 63.34; H, 5.56; N, 12.73. FAB mass: m/z 341. Selected IR peaks with tentative assignments (ν_{max}, cm^{-1}): 3457 (O–H), 2963 (C–H), 1635 (C═N Schiff base coupled to the aromatic ring), 1011 (C–O phenol), 978(V=O).

Cell culture and transfection

3T3-L1 and HEK-293 cells were obtained from the Korean Cell Line Bank (Seoul, South Korea) and cultured in Dulbecco's modified Eagle's medium (DMEM) , supplemented with 10% fetal bovine serum, 100 μg/ml penicillin and 100 μg/ml streptomycin at 37 °C

View Article Online
DOI: 10.1039/C6RA11111D

in a humidified atmosphere of 5% CO_2. HEK-293 cells were kept overnight in serum-free DMEM without antibiotics, and transfected at 50-70% confluence with 1-5 μg of pB-GLUT4myc7-GFP plasmid using lipofectamine-3000 (Invitrogen, CA, USA). Cells were grown for 48 h, and the medium was replaced by DMEM containing FBS and antibiotics. GLUT4-GFP expression was monitored by a fluorescence microscope.

Glucose uptake assay

3T3-L1 cells were seeded in 12-well cell culture plates (1×10^6 cells per well) and grown overnight. Cells were then differentiated into adipocytes.[12] The adipocytes were then kept in serum-free DMEM without antibiotics for 4 h, and treated with 100 nM of insulin or different concentrations of VOTP (10 nM, 50 nM, 100 nM, and 200 nM) at 37 °C for 15 min. Each well was washed twice with Krebs Ringer Phosphate buffer (KRP buffer). Then, cells were incubated with 100 μM of 2-[N-(7-nitrobenz-2-oxa-1, 3-diazol-4-yl)amino]-2- deoxy-D-glucose (2-NBDG) at 37 °C for 10 min. After removal of the incubation medium, the cells were washed three times with ice-cold PBS. The glucose uptake by the cells was detected by measuring the fluorescent intensity of 2-NBDG. Images were acquired by a fluorescence microscope (IX73, Olympus, Tokyo, Japan) using 488 nm excitation wavelength and 525 nm emission wavelength. Images were processed using MetaMorph software, Version 7.1.3.0.

TIRF imaging studies

HEK-293 cells were grown on coverslips in 6-well cell culture plates overnight. Cells were then transfected with 1-5 μg of pB-GLUT4myc7-GFP plasmid using lipofectamine-3000 (Invitrogen, CA, USA) and allowed to grow for 48 h. Cells were pretreated with VOTP or aspirin for 30 min in growth medium prior to TNF-α treatment and were treated

View Article Online
DOI: 10.1039/C6RA11111D

with 10 ng/ml of TNF-α for 5 h. Insulin was treated for 30 min after TNF-α treatment. Coverslips were then taken off and used for imaging of GFP fluorescence by TIRF microscope (lg-TIRFM, TIRF Labs, NC, USA). All the images were taken at 20X magnification and image analysis was performed using MetaMorph software, Version 7.1.3.0.

Qdot-Ab conjugation and imaging

The Abs against phospho forms of GSK-3β, JNK, IRSser, FOXO, and IRStyr were conjugated to Qdot525, QDot565, Qdot625, Qdot655, and Qdot705, respectively, according to Tak et al.[13] HepG2 cells were fixed in 4% formaldehyde, washed with PBS, and treated with 0.2% saponin followed by washing. The cells were incubated with the diluted Qdot-Ab conjugates at room temperature for 1 h. The cells were then washed with PBS, and Qdot emission was detected using an Acusto optic tunable filter (AOTF) (AOTF, TEAF10-0.45-0.7-S, Brimrose Corporation, MD, USA) and a fluorescence microscope (IX71, Olympus, Tokyo, Japan). All the images were taken at 20X magnification and imaging analysis was performed using MetaMorph software, Version 7.1.3.0.

Statistical analysis

Each experiment was repeated three times. The statistical analysis was performed by one-way analysis of variance (ANOVA) to compare the means of two or more treatment groups, followed by post-Hoc multiple comparisons by the Tukey method. The difference was considered as significant when $p < 0.05$.

Results and discussion

View Article Online
DOI: 10.1039/C6RA11111D

Type II diabetes mellitus is a chronic disease, the rate of which increased dramatically during the last two decades. The medicine currently used in the treatment of T2DM may cause a number of detrimental side effects. On the other hand, insulin treatment is expensive, and regular injection strategies are frequently painful to patients. Hence, it is important to screen for insulin mimetic substances for effective treatment strategies against T2DM. Recent studies have identified a strong correlation among obesity, inflammation, and T2DM. Inflammatory mediators like TNF-α play significant role in the onset and progression of T2DM. Available drugs and phytochemicals show promising insulin mimetic action. However, they are administered in high doses that cause other undesirable symptoms. A molecule possessing insulin mimetic activity along with anti-inflammatory action activities may constitute a suitable alternative in treating T2DM. Earlier studies have reported that vanadium oxo complexes possess insulin-mimetic activities. Vanadium metal salts and their complexes are well studied in catalytic and biological applications, such as antimicrobial, antitumor, and anti-leukaemia therapy.[14,15] Vanadium can form complexes with Schiff base ligands in different oxidation states to form compounds possessing high stability and serve important biological applications as insulin mimetic agents.[16] Schiff base ligands are called “privileged ligands”, and they are easily prepared by condensation between an aldehyde and primary amine. We envisaged that choosing pydridoxal hydrochloride and tryptamine would contribute greatly in enhancing antidiabetic and anti-inflammatory properties. Pyridoxal 5′-phosphate (PLP) and pyridoxamine (PM), the active forms of vitamin-B6, are known to inhibit the formation of advanced glycation end-products (AGEs), and hence have been explored as active pharmaceutical agents for the treatment of diabetes.[17] Recent studies demonstrated that PLP can restrict the progression of diabetic nephropathy, and is considered to constitute a promising candidate for the treatment of age-related diabetic

View Article Online
DOI: 10.1039/C6RA11111D

complications.[18] Similarly, tryptamine-based compounds were studied for anti-inflammatory activities. Thus, it may be likely that utilizing pyridoxal hydrochloride and tryptamine in forming a Schiff base ligand can produce a bifunctional activity along with vanadium.

Synthesis of Vanadium (IV) complex of pyridoxylidenetryptamine Schiff base complex (VOTP)

Scheme (Fig. 1B (ii)) shows the one-pot synthetic method utilized in the current study for the preparation of vanadyl Schiff base complex (VOTP). A complexation reaction was performed by the addition of vanadyl metal salt (VO^{2+}) to the pyridoxal hydrochloride and tryptamine in the presence of sodium acetate and the reaction mixture was refluxed for 12 h. The green powder was isolated and washed with diethyl ether to obtain a vanadium (IV) complex of pyridoxylidenetryptamine Schiff base (VOTP) in 50% yields.

Structural and spectral characterization of TPL and VOTP

The synthesized pyridoxylidenetryptamine Schiff base ligand (TPL) and VOTP were fully characterized by FAB mass, FT-IR, electronic absorption spectroscopy, ^{1}H NMR, and TGA/DSC. The FAB mass spectrum of TPL showed a molecular ion peak [M+1] at m/z 310 that revealed the formation of Schiff base ligand (supporting information Fig. S1). IR spectrum analysis was performed in the range of 4000-400 cm^{-1}. The azomethine –C=N band appeared at 1495 cm^{-1} in the TPL ligand (supporting information Fig. S3). This confirms the formation of an imine bond during the condensation reaction of pydridoxal hydrochloride and tryptamine. Further validation was achieved by ^{1}H NMR spectrum, which showed a peak at δ=7.95 ppm for –CH=N in the TPL ligand (supporting information Fig. S4). Similar characterization analyses were conducted for the VOTP complex. The complex formation was verified by FAB mass analysis. The FAB mass spectrum of charged species of VOTP showed a peak at m/z 341

View Article Online
DOI: 10.1039/C6RA11111D

(supporting information Fig. S2). IR analysis of the VOTP complex showed a band at 1622 cm^{-1} for azomethine –C=N and stretching vibration of the V=O bond at 978 cm^{-1}, indicating coordination of vanadyl ion to the Schiff base. However, due to the paramagnetic (d^1 system) nature of vanadyl (IV), it was not feasible to record the ^1H NMR spectrum for the VOTP complex.[19-20]

Electronic absorption spectrum of TPL and VOTP

Figure 2 shows the electronic absorption spectra for the Schiff base ligand and its complex. The spectra were measured in DMSO. The electronic spectra of TPL and VOTP exhibited a band at 284 nm, typical of n-π* transition. It also revealed bands at 348 nm and 365 nm for ligand and complex, respectively, which may be attributable to the ligand-based π-π* transition. The π-π* transition of VOTP showed a red shift of 17 nm compared with that of the ligand. This suggests the coordination of metal ion to the ligand.

Thermal analysis

Thermogravimetric analysis (TGA) and differential scanning calorimetry (DSC) were carried out to determine the thermal stability of the VOTP complexes. The TGA/DSC measurement for the VOTP complex was performed in the range of ambient temperature to 800^0C at a heating rate of 10^0C per min. The obtained TGA/DSC curves are shown in Fig. 3. The TGA profile exhibited three major distinctive decomposition steps. The first decomposition was observed between room temperature and 120^0C, which corresponded to a loss of water molecules in the VOTP complex. The second decomposition step was observed around 253^0C, which may be due to the loss of the whole complex molecule. The third decomposition step was observed at 300 to 450^0C, which may have arisen from the phase transformation of TPL ligand moiety. The total mass loss value was 45.35%. The DSC curve showed one major peak and six small peaks. Below

View Article Online
DOI: 10.1039/C6RA11111D

200^{0}C, three thermal decomposition curves were observed, respectively, at 50^{0}C, 100^{0}C, and 150^{0}C, which corresponded to the loss of external water molecules. The peak around 253^{0}C might be due to the decomposition of the VOTP complex. The broad DSC peak between 300 and 450◦C corresponded to calcination of the organic ligand TPL.

Insulin mimetic action of VOTP

We aimed at studying the GLUT4 translocation to the plasma membrane, which may be considered as a marker to assess the insulin mimetic potential of compounds. The traditional wet lab methods for the analysis of insulin-mimetic drugs suffer from the disadvantage of non-specific signal intensities. Confocal microscopic analysis of fluorescent GLUT4 fusion proteins or the Q-dot approach is insufficient to quantify the exact levels of GLUT4 translocation due to the high noise generated from intracellular signalling. TIRF is a relatively new approach in studying GLUT4 translocation. The fluorescent intensities detected at the evanescent field specifically correspond to the membrane-associated molecules without any intracellular noise detection. As GLUT4 translocation is the major issue in addressing insulin signalling and T2DM, effective visualization and quantitative analysis of localization results may be an effective way to screen for anti-diabetic and anti-inflammatory drugs. For optimization of VOTP concentration for further experiments, the cellular glucose uptake was determined by measuring intracellular glucose content in 3T3-L1 adipocytes treated with different concentrations of VOTP. The maximum glucose uptake was observed at 100 nM concentration of VOTP (Fig 4A v). Usually, differentiated adipocytes or myotubes are used to study GLUT4 translocation. In this study, to monitor the GLUT4 translocation we used HEK-293 cells which are also widely used to study the translocation of GLUT-4 from the cytoplasm to the plasma membrane. Previous reports revealed that HEK-293 cells were effectively translocating the GLUT-4 to the membrane by

View Article Online
DOI: 10.1039/C6RA11111D

adopting similar signalling cascades observed in adipocytes and myotubes.[21-23] The pB-GLUT4myc7-GFP construct was transfected into HEK-293 cells. The retroviral vector pB contained a human GLUT4 cDNA, and c-myc epitope tag fused with the green fluorescent protein (GFP) coding sequence. A stable expression level of the GLUT4 reporter protein by the transfected cells was monitored by the detection of fluorescence emitted by GFP. The transfection efficiency was found to be almost 76%. The result for glucose uptake was further confirmed by monitoring GLUT4 translocation by TIRF with different dosage treatment of VOTP on HEK-293 cells (Fig 4B). VOTP showed the potential of insulin mimetic activities even at nanomolar treatment ranges. We optimized the dosage (100 nM VOTP) (Fig 4B iv) for further studies in the IR model.

Anti-inflammatory potential of VOTP

In order to elucidate the role of VOTP during inflammation-induced IR, we selected the TNF-α induced IR model of HEK-293 cells. Inflammation –induced IR state was already well established methodology to study the glucose uptake and other metabolism associated with glucose, which was well documented in adipocyte tissues and other cell types majorly contributing the glucose metabolism such as HepG-2 cells.[24,25] TNF-α –induced IR state was also previously reported in HEK-293 cells. [26,27] The transfected cells were subjected to starvation conditions before treatment with TNF-α or stimulation with insulin and/or VOTP. To confirm the anti-inflammatory potential of VOTP, we compared the fluorescent signal intensities of GLUT4-GFP, as a measure of GLUT4 translocation to the plasma membrane, obtained by TIRF microscopy from different experimental groups. Cells treated with TNF-α completely blocked GLUT4 translocation. (Fig 5A i). Whereas, VOTP treatment along with the induction of IR by TNF-α; significantly induced GLUT4 translocation. In addition, a marked increase in the level of

View Article Online
DOI: 10.1039/C6RA11111D

GLUT4 translocation with respect to increase in VOTP dosage was also observed. (Fig 5A ii-v). In another set of experiments, the cells were pretreated with VOTP in order to assess its anti-inflammatory potential during TNF-α induced IR. TIRF images showed that TNF-α induced IR state completely inhibited the insulin signalling (Fig 3B i). Interestingly, the pre-treatment of VOTP prior to IR induction effectively restored the insulin signalling in TNF-α treated HEK-293 cells, the extent of which increased with increase in VOTP concentration and attained the maximum level at 100 nM of VOTP pretreatment (Fig 5B ii-v).Equal dosage of VOTP and insulin, induced a comparable extent of GLUT4 translocation (Fig 6A).

To compare the anti-inflammatory potential of VOTP, we used aspirin, a known anti-inflammatory drug, during IR. TIRF results showed that VOTP (100 nM) pre-treatment could induce significant extent of GLUT4 translocation in absence of insulin even after the induction of IR (Fig 6B iii). we also observed that, VOTP (100 nM) pre-treatment exhibited much better ability in restoring insulin signalling and GLUT4 translocation (Fig 6B v), even at much lower concentrations in comparison to aspirin treatment (100 μM) (Fig 6B iv). The mode of activation of the Insulin mimetic drugs is independent of IRS-tyrosine kinase (IRSTK). Instead, they are processed via activation of phosphatidylinositol-3-kinase (PI3K) which, in turn, activates IRS by phosphorylation of its tyrosine moiety. We applied wortmannin, a potent inhibitor of PI3K, to assess the role of the kinase in VOTP induced IRS activation. Wortmannin pretreatment decreased the extent of GLUT4 translocation; however it could not completely block the GLUT4 translocation of VOTP-pretreated cells prior to IR induction (Fig 6B vi). In general, PI3K inhibition hampers the action of insulin mimetic drugs. Accordingly, the insulin mimetic action of VOTP should be unable to induce GLUT4 translocation and intracellular glucose uptake. Hence, we explored that VOTP may act via a different mechanism to stimulate GLUT4

View Article Online
DOI: 10.1039/C6RA11111D

translocation and to restore insulin signalling in our experimental model. The most evident mechanism may be its anti-inflammatory action, which triggers the reactivation of IRSTK to phosphorylate the IRS tyrosine moiety. This idea was obviously supported by the data of wortmannin-treated cells, in which VOTP treatment induced significant GLUT4 translocation (Fig 6B vi).

To further confirm the anti-inflammatory potential of VOTP, the activity levels of certain intracellular kinases, which are related to inflammation-induced IR were determined by high-content monitoring using QDot antibody (Ab) conjugates. High-content monitoring does not require cell lysis, and several biomolecules can be quantified concurrently from a single sample in a single run. High fluorescent intensity of QDots leads to high resolution images and accuracy in quantification. Generally, TNF-α induces IR via the phosphorylation and activation of JNK-1. It also triggers the inactivation of glycogen synthase kinase (GSK), decreases the level of phosphorylated FOXO1, and inhibits the phosphorylation and subsequent activation of IRS tyrosine (IRStyr).[28] In T2DM, adipocytes are critically involved in the establishment of inflammatory state of the system by secreting various inflammatory cytokines including TNF-α in association with tissue infiltrating macrophages. However, in liver and muscle cells the glucose uptake was reported to be impaired due to the insulin resistance established by inflammatory state. [29, 30] Hence, we used HepG2 cells to study the anti-inflammatory potential of VOTP and its role in regulating the intracellular kinases associated with inflammation induced IR state. HepG2 cells are a liver cell (Meijer et al., 2015). HepG2 cells pretreated with VOTP followed by IR induction significantly reduced the level of phosphorylated JNK-1 with a concomitant increase in the levels of phosphorylated forms of IRStyr and GSK3β (Fig 7A iv). In addition, VOTP produced a marked increase in the levels of phosphorylated FOXO, thus

View Article Online
DOI: 10.1039/C6RA11111D

stopping gluconeogenesis, which otherwise depends on the level of non-phosphorylated FOXO (Fig 7A iv). The low levels of the phosphorylated form of IRS serine (IRSser) and high levels of phosphorylated IRStyr (Fig 7A iv) confirmed that VOTP pretreatment caused the activation of IRSTK, which is otherwise deactivated during inflammation-induced IR. The applied VO complex plays a bifunctional role in maintaining normal glucose homeostasis. Specifically, it may: (i) act by activating IRS-tyrosine kinase during the inflamed condition, which reflects its anti-inflammatory potential; or (ii) act by the PI3K dependent pathway, which reflects its insulin mimetic potential. Inflammation plays a major role in the onset and progression of T2DM. In T2DM, the activation of IRS is blocked by the inactivation of IRSTK that otherwise phosphorylates and activates IRStyr for effective insulin signalling. Thus, an effective way to treat T2DM is to utilize anti-inflammatory drugs to restore insulin signalling. Moreover, insulin-mimetic drugs are also applied to maintain normal glucose homeostasis. The synthesized vanadyl complex possesses both of these properties and can constitute a suitable alternative to traditional drugs. The compound is effective at the nanomolar treatment range that is generally non-toxic to living cells. The screening system to quantify the GLUT4 translocation involving a combination of an inflammation-induced IR cellular model and TIRF demonstrates effectiveness in analysing such compounds in a convenient manner with high precision.

Conclusions

The current study constitutes perhaps the pioneering report of a synthesized vanadyl complex possessing insulin-mimetic and anti-inflammatory properties together. As the complex is highly active at very low doses, it may find a suitable role as an alternative

View Article Online
DOI: 10.1039/C6RA11111D

over traditional drugs for treating T2DM. Further research is necessary in order to assess the adverse effects of this complex, if any, in animal models.

Acknowledgements

We are grateful to the Research Institute of Pharmaceutical Sciences at Seoul National University for providing experimental equipment. This work was supported by National Research Foundation of Korea (NRF) grant funded by the Ministry of Education, Science and Technology (MEST) (2015R1A2A1A05001842).

Declarations of interest

The authors declare no competing financial interests.

References

1 Z. Zhang, M. Zhao, Q. Li, H. Zhao, J. Wang, and Y. Li, *FEBS Lett*. 2009, 583, 470.

2 P.A. Kern, Ranganathan, S., Li, C., Wood, L. and Ranganathan, G, *Am. J. Physiol Endocrinol. Metab*, 2001, 280, E745.

3 H. Kanety, R. Feinstein, M. Z. Papa, R. Hemi, and A. Karasik, *J.Biol. Chem,* 1995, 270, 23780.

4 J. M. Stephens, J. Lee, and P. F. Pilch, *J. Biol. Chem,* 1997, 272, 971.

5 E. Carvalho, P. A. Jansson, I. Nagaev, A. M. Wenthzel, and U. Smith, *Faseb. J.* 2001, 15, 1101.

6 V. Rotter, I. Nagaev, and U. Smith, *J.Biol. Chem,* 2003, 278, 45777.

View Article Online
DOI: 10.1039/C6RA11111D

7 A. Nohara, S. Okada, K. Ohshima, J. E. Pessin, and M. Mori, *J.Biol. Chem,* 2011, 286, 33457.

8 M. Z. Mehdi, S. K. Pandey, J. F. Theberge, and A. K. Srivastava, *Cell. Biochem.Biophys,* 2006, 44, 73.

9 S. H. Li, and J. H. McNeill, *Mol. Cell. Biochem*. 2001, 217, 121.

10 P. Lanzerstorfer, V. Stadlbauer, L. A. Chtcheglova, R. Haselgrubler, D. Borgmann, J. Wruss, P. Hinterdorfer, K. Schroder, S.M. Winkler, O. Hoglinger, and J. Weghuber, *Br. J. Pharmacol*. 2014, 171, 5237.

11 T. Mukherjee, J. Costa Pessoa, A.Kumar, A.R. Sarkar *Dalton Trans*. 2013 42(7):2594.

12 K. Zebisch, V. Voigt, M. Wabitsch, and M. Brandsch, *Anal. Biochem*, 2012, 425, 88-90.

13 Y. K. Tak, P. K. Naoghare, B. J. Kim, M. J. Kim, E. S. Lee, and J. M. Song, *Nano Today*. 2012, 7, 231.

14 A. P. Mishra, and M. Soni, *Met Based Drugs.* 2008, 2008:875410.

15 P. Noblia, M. Vieites, B.S. Parajon-Costa, E.J. Baran, H. Cerecetto, P. Draper, M. Gonzalez, O. E. Piro, E. E. Castellano, A. Azqueta, A. Lopez de Cerain, A. Monge-Vega, and D. Gambino, *J. Inorg. Biochem.* 2005, 99, 443.

16 H. Han, L. Lu, Q. Wang, M. Zhu, C. Yuan, S. Xing, and X. Fu, *Dalton Trans*. 2012, 41, 11116.

17 T. Ishida, K. Hatta, S. Yamashita, M. Doi, and M. Inoue, *Chem. Pharm. Bull (Tokyo)*, 1986, 34, 3553.

18 S. Nakamura, H. Li, A. Adijiang, M. Pischetsrieder, and T. Niwa, *Nephrol. Dial. Transplant*. 2007, 22, 2165.

19 H. Hagen, A. Barbon, E. E. van Faassen, B.T. G. Lutz, J. Boersma, A. L. Spek, and G. K

View Article Online
DOI: 10.1039/C6RA11111D

oten, *Inorg.chem.* 1999, 38, 4079.

20 B. Banik, K. Somyajit, G. Nagaraju and A.R. Chakravarty, *Dalton Trans.* 2014, 43(35):1 3358.

21 F. Liu, Q. Dallas-Yang, G. Castriota, P. Fischer, F. Santini, M. Ferrer, J. Li, T. E. Akiyama, J. P. Berger, and B. B. Zhang, *Biochem. J.* 2009, 418, 413.

22 S. T. Yan, C. L. Li, H. Tian, J. Li, Y. Pei, Y. Liu, Y. P. Gong, F. S. Fang, and B. R. Sun, *Mole. Cell. Biochem.* 2014, 397, 45.

23 R. Augustin, J. Riley, and K. H. Moley, *Traffic.* 2005, 6, 1196.

24 M. Hiromura, A. Nakayama, Y. Adachi, M. Doi, and H. Sakurai, *J. Biol. Inorg. Chem*. 2007, 12, 1275.

25 K. Tordjman, K. Leingang, and M. Mueckler, *Biochem. J.* 1990, 271, 201.

26 K. Meijer, R. J. Vonk, M. G. Priebe, and H. Roelofsen, *Food. chem*. 2015, 166, 158.

27 H. C. Chuang, W. H. Sheu, Y. T. Lin, C. Y. Tsai, C. Y. Yang, Y. J. Cheng, , P. Y. Huang, J. P. Li, L. L. Chiu, and X. Wang, *Nat .commun,* 2014, 5, 4602.

28 M. J. Kim, S. Rangasamy, Y. Shim, JM.Song. *J. Nanobiotechnology*. 2015, 13, 4.

29 H. Tilg, and A. R. Moschen, , 2008. *Mol. Med*, 2008, 14(3-4), 222.

30 M. R. Maradana, R. Thomas, and B. J. O'Sullivan, , 2013. *Mol. Nut. Food. Res,* 2013, 57, 1550.

Figure captions

Figure 1. Schematic representation: (A) Insulin signaling pathway and GLUT4 translocation. Binding of insulin to its receptor induces phosphorylation, followed by the recruitment of IRS, which ultimately leads to the translocation of GLUT4-containing vesicles from cytosol to the

View Article Online
DOI: 10.1039/C6RA11111D

plasma membrane. TNF-α blocks the phosphorylation and activation of insulin receptor to deactivate the downstream kinases and blocks GLUT4 translocation and glucose uptake by cells. VOTP plays an anti-inflammatory role against TNF-α induced insulin resistance. Cells expressing GLUT4-myc-GFP were grown on coverslip glass. Fluorophores localized at the evanescent field (plasma membrane) only, could be visualized by TIRF microscopy. **(B) (i)** Chemical structure of the Schiff base ligand (TPL) and **(ii)** One-pot synthesis of bifunctional (pyridoxylidinetryptamine) vanadium (IV) complex (VOTP).

Figure 2. UV-Visible Absorption spectra of TPL and VOTP.

Figure 3. TGA/DSC profile curves of VOTP complex.

Figure 4. (A) Effect of different concentrations of VOTP on glucose uptake by differentiated 3T3-L1 adipocytes. Insulin was used to compare the insulin-mimetic efficacy of VOTP. (i) control; (ii) insulin (100 nm); (iii) VOTP (10 nm); (iv) VOTP (50 nm); (v) VOTP (100 nm); (vi) VOTP (200 nm). (vii) shows the respective fluorescence intensities that correspond to the amount of glucose uptake. (B) **Quantification of VOTP-induced GLUT4 translocation in HEK-293 cells by using TIRF microscopy** (i) control; (ii) VOTP (10 nm); (iii) VOTP (50 nm); (iv) VOTP (100 nm); (v) VOTP (200 nm). (vi) Shows the respective fluorescence intensities that correspond to the amount of glucose uptake in HEK-293 cells in response to the different concentration of VOTP. The data of insulin and VOTP treated groups were compared with those of the control group. ***p <0.001 and **p <0.01 vs control.

Figure 5. (A) Effect of VOTP on GLUT4 translocation during TNF-α induced IR state in the HEK-293 cells. (i) Control;(ii) VOTP (10 nm); (iii) VOTP (50 nm); (iv) VOTP (100 nm); (v) VOTP (200 nm). (vi) shows the respective fluorescence intensities that correspond to the amount of GLUT-4 translocation. The data of (TNF-α+VOTP) treated groups were compared

View Article Online
DOI: 10.1039/C6RA11111D

with those of the TNF-α treated group. **(B) Effect of pretreatment of VOTP on insulin signalling as assessed by measuring GLUT4 translocation during TNF-α induced IR state.** (i) control; (ii) VOTP (10 nm); (iii) VOTP (50 nm); (iv) VOTP (100 nm); (v) VOTP (200 nm). (vi) Shows the respective fluorescence intensities that correspond to the amount of glucose uptake. The data of (VOTP+TNF-α) treated groups were compared with those of the TNF-α treated group. *p<0.05; **p<0.01; ***p<0.001 vs control.

Figure 6. (A) Comparison of the insulin-mimetic potential of VOTP. (i) control; (ii) insulin (100 nm); (iii) VOTP (100 nm). (iv) Shows the representative histogram corresponding to the fluorescence intensities of GFP as a measure of GLUT4 translocation. The data of insulin and VOTP treated groups were compared with those of the control group. **(B) Assessment of the anti-inflammatory potential of VOTP.** (i) control; (ii) TNF-α+insulin; (iii) VOTP (100 nm)+TNF-α; (iv) aspirin (100 μM)+TNF-α+insulin; (v) VOTP (100 nm)+TNF-α+insulin; (vi) wortmannin+VOTP (100 nm)+TNF-α+insulin. Cells were treated with VOTP or aspirin prior to TNF-α treatment. Insulin (100 nm) was applied after the TNF-α treatment. (vii) Shows the representative histogram corresponding to the fluorescence intensities of GFP as a measure of GLUT4 translocation. The data of the control group were compared with those of the (TNF-α+insulin) treated group. The data of TNF-α+VOTP/aspirin treated groups were compared with those of the (TNF-α+insulin) treated group. *p<0.05; ***p<0.001 vs control

Figure 7. (A) High-content multicolor cellular images showing simultaneous monitoring of the upregulation/downregulation of insulin downstream signal molecules p-GSK3β, p-JNK1, pIRSser, p-FOXO1, and p-IRStyr. (i) control; (ii) insulin; (iii) aspirin (100 μM)+TNF-α+insulin; (iv) VOTP (100 nm)+TNF-α+insulin. HepG2 cells were treated with VOTP or aspirin prior to TNF-α treatment. Insulin was applied after the TNF-α treatment. The images

View Article Online
DOI: 10.1039/C6RA11111D

(10X) were acquired using a fluorescent microscope (Model) equipped with AOTF (Company).

(B) Representative histogram corresponding to the fluorescence intensities of QDots. The data of the control group were compared with those of the TNF-α+insulin treated group. The data of TNF-α+VOTP/aspirin treated groups were compared with those of the TNF-α+insulin treated group. **p<0.01; ***p<0.001 vs control.

Figure 1

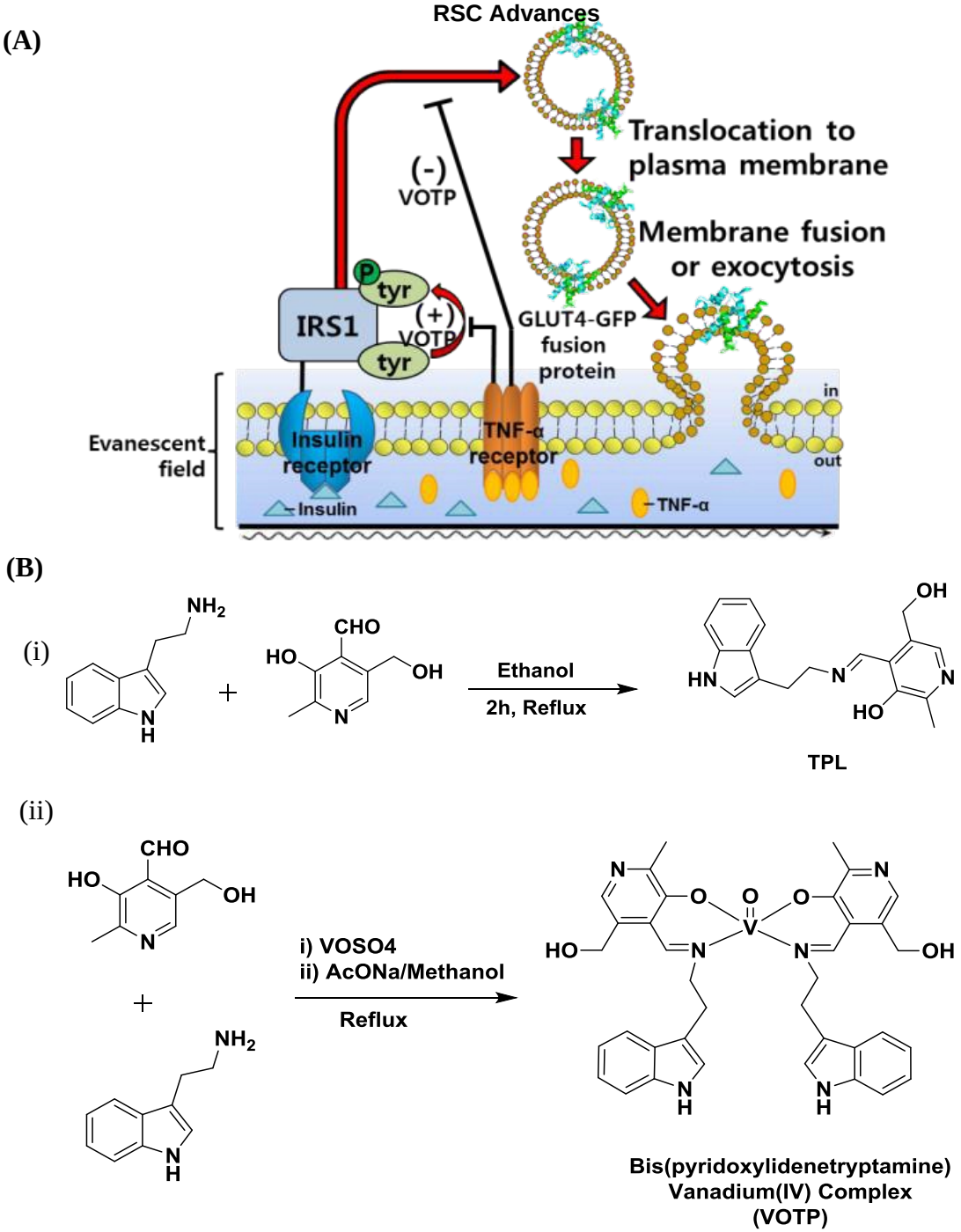

Figure 2

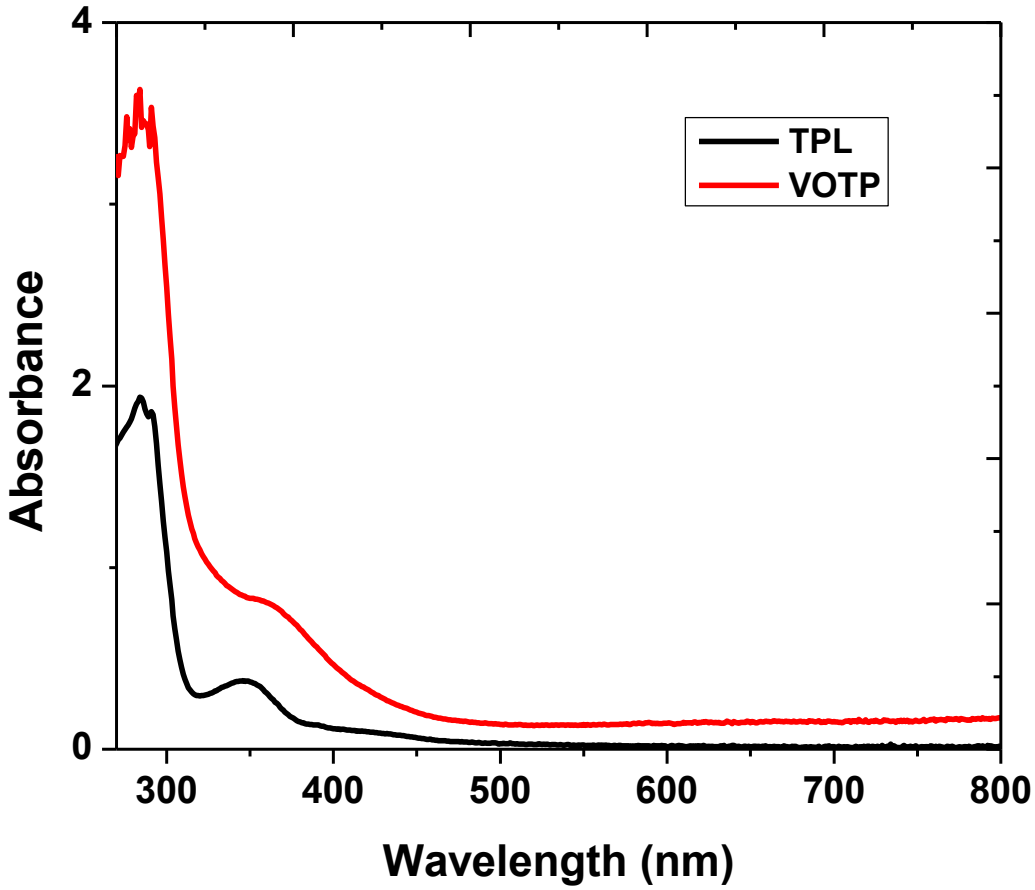

Figure 3

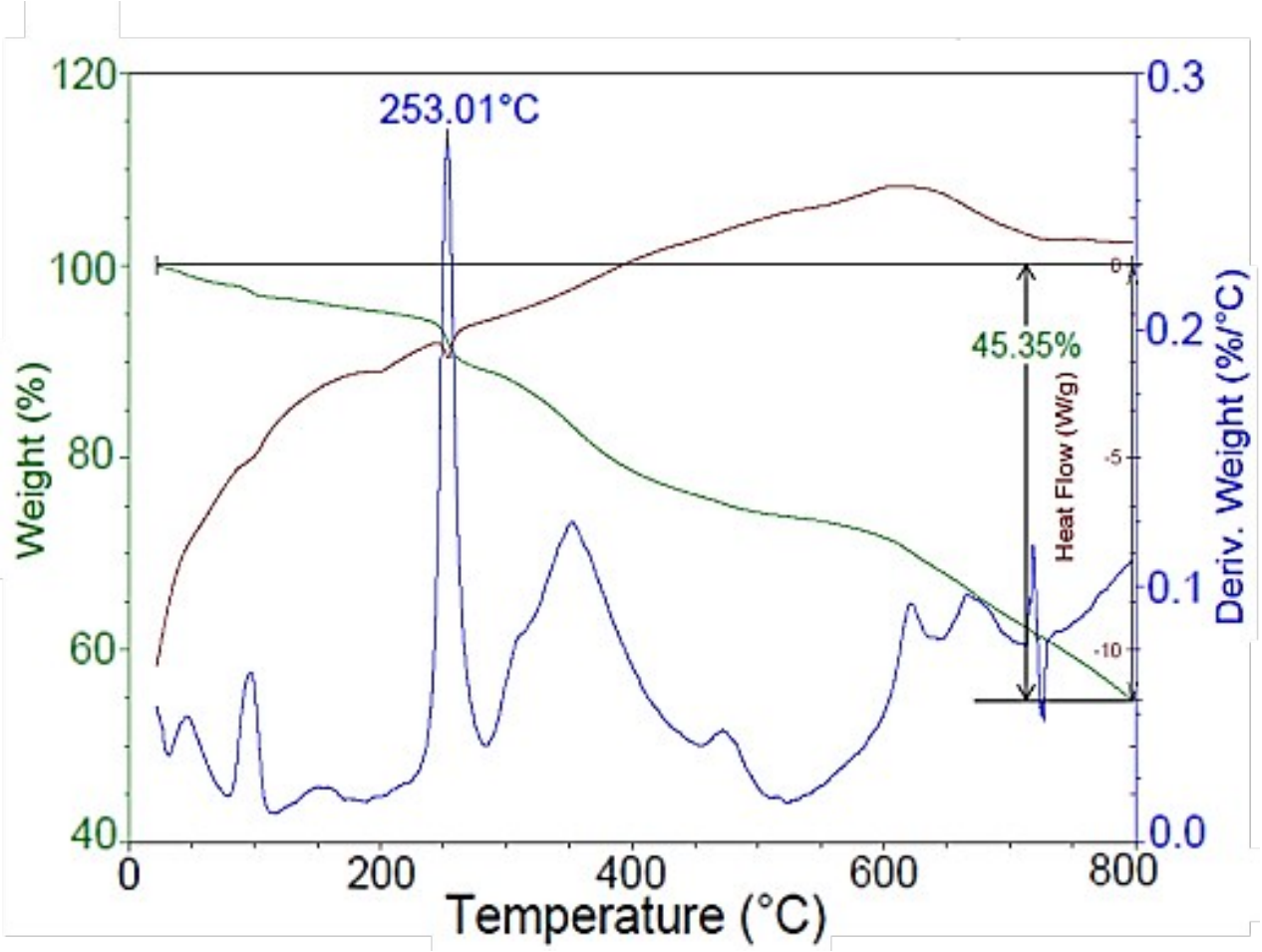

Figure 4

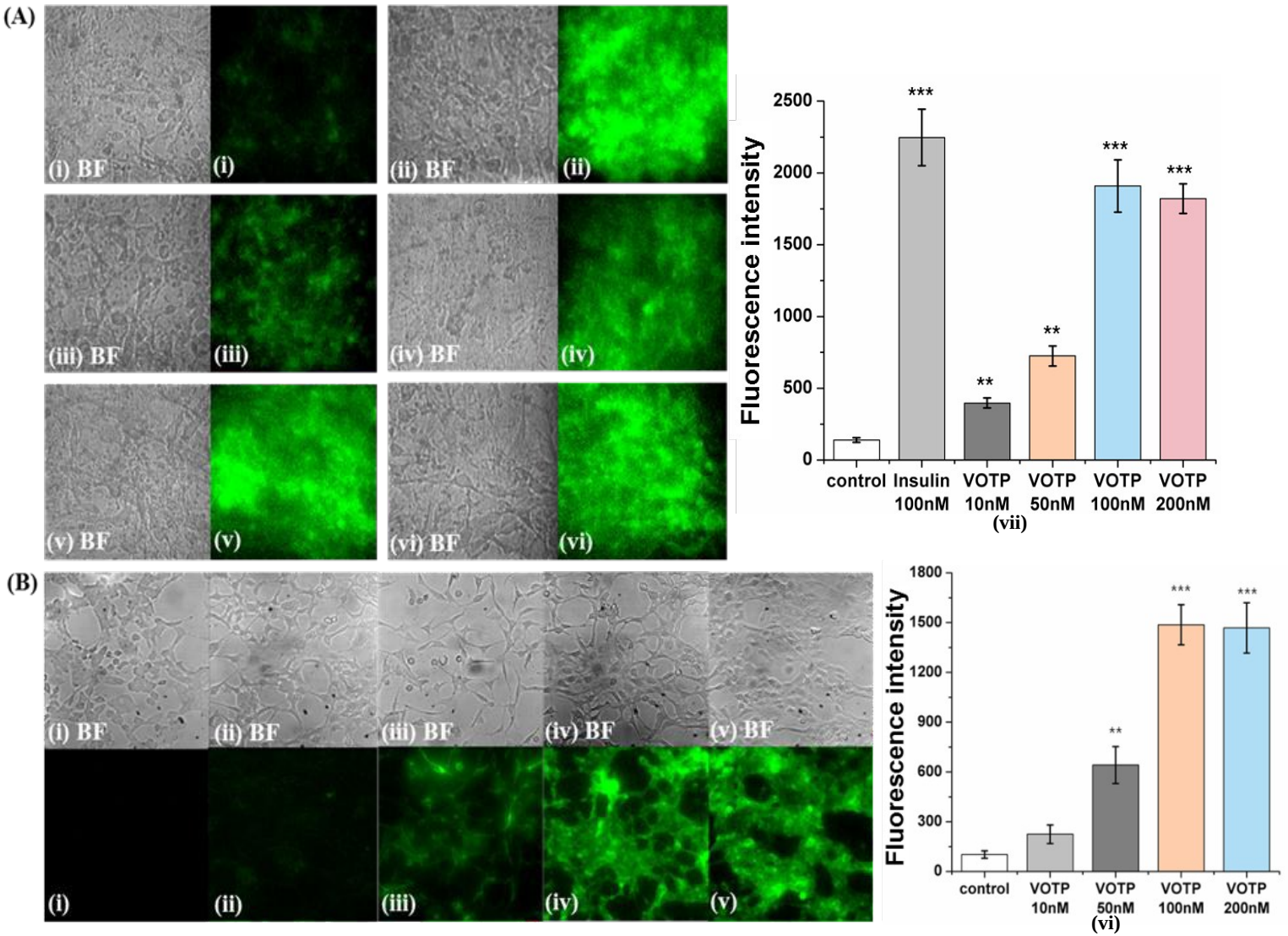

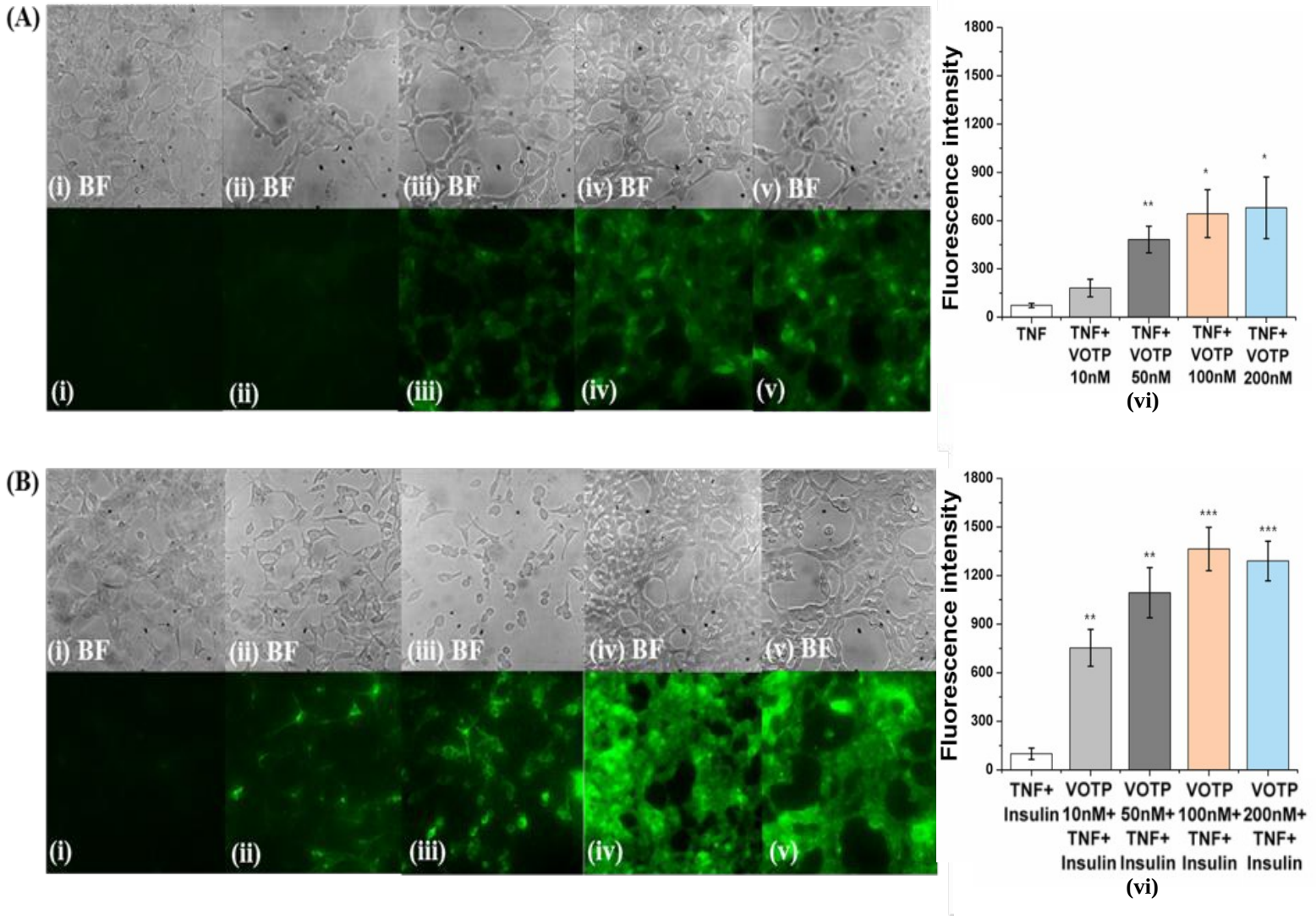

Figure 6

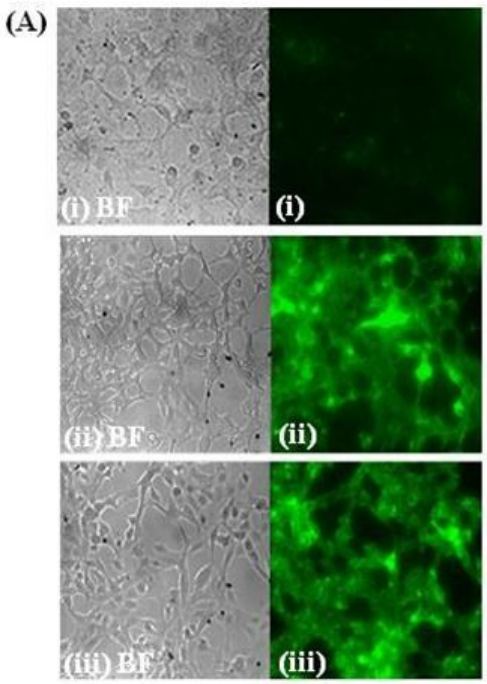

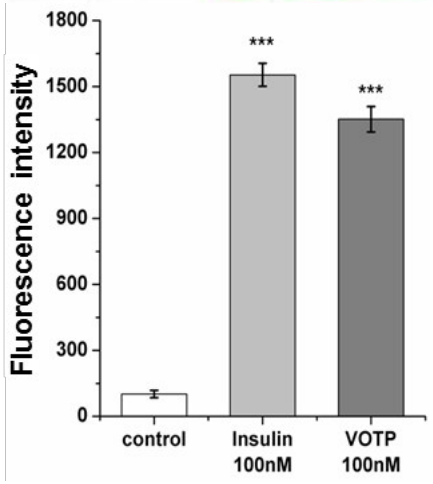

(iv)

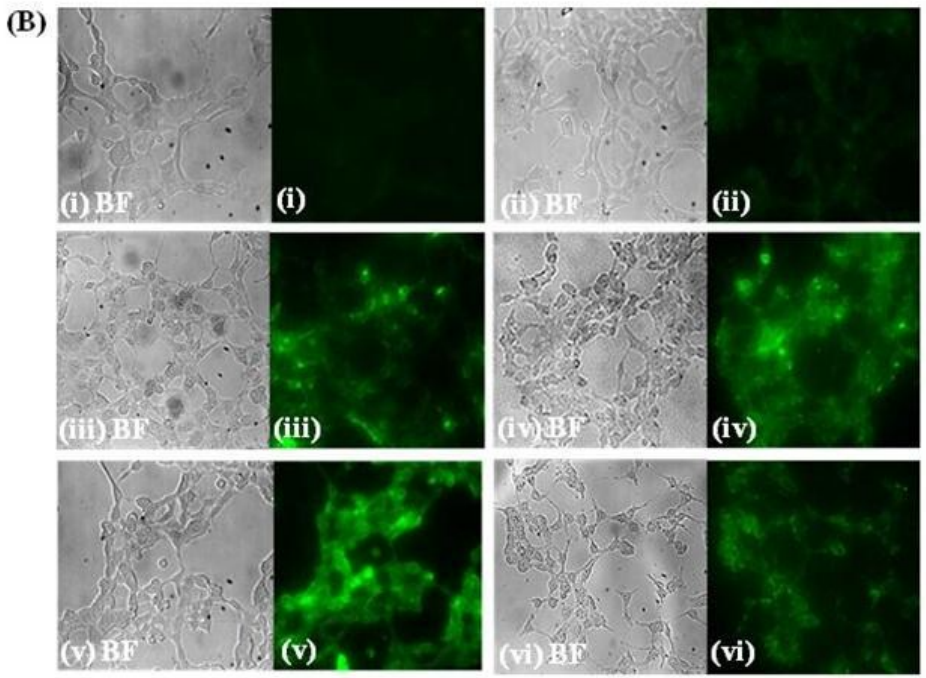

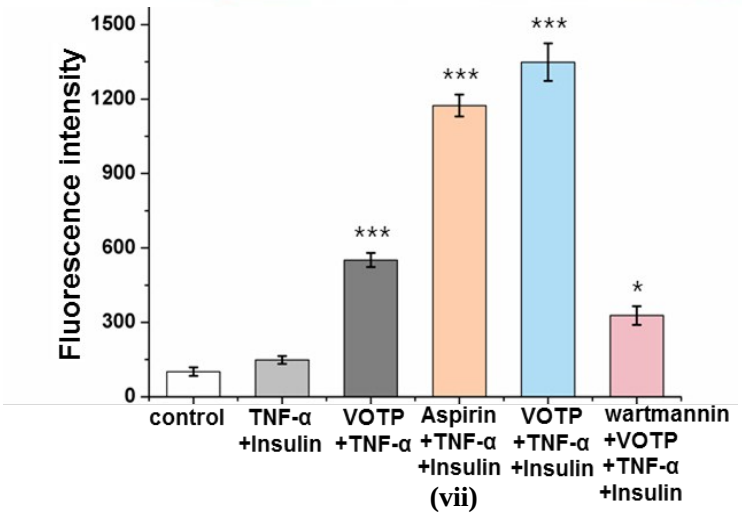

(vii)